IEEE Photonics Journal
An IEEE Photonics Society Publication

Open Access

Multicarrier Approaches for High-Baudrate Optical-Fiber Transmission Systems With a Single Coherent Receiver

Volume 9, Number 2, April 2017

Tu T. Nguyen
Son T. Le
Qinwei He
Ludo V. Compernolle
Marc Wuilpart
Patrice Mégret

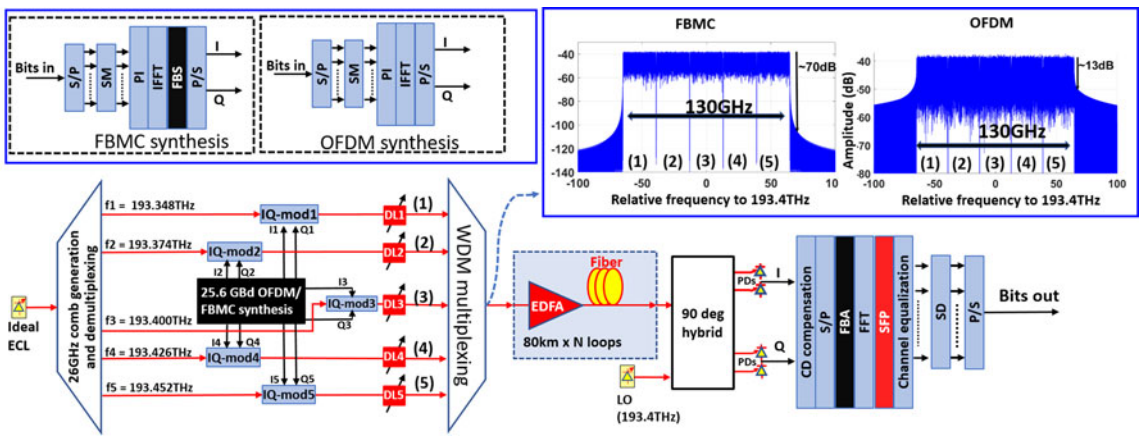

DOI: 10.1109/JPHOT.2017.2672041
1943-0655 © 2017 IEEE

Multicarrier Approaches for High-Baudrate Optical-Fiber Transmission Systems With a Single Coherent Receiver

Tu T. Nguyen,[1,4] Son T. Le,[2] Qinwei He,[3] Ludo V. Compernolle,[4] Marc Wuilpart,[1] and Patrice Mégret[1]

[1]Faculté Polytechnique—Université de Mons, Mons 7000, Belgium
[2]Nokia Bell Labs, Stuttgart 70435, Germany
[3]Institute for Theoretical Information Technology, RWTH Aachen University, Aachen 52056, Germany
[4]Proximus SA, Brussels 1030, Belgium

DOI:10.1109/JPHOT.2017.2672041

Manuscript received January 17, 2017; revised February 12, 2017; accepted February 16, 2017. Date of publication February 20, 2017; date of current version March 10, 2017. This work was supported by the EU Project ICONE under Grant #608099, in collaboration with Proximus SA, Belgium. Corresponding author: T. Nguyen (e-mail: tuthanh.nguyen@student.umons.ac.be).

Abstract: In this paper, we show the remarkable timing error (TE) and residual chromatic dispersion (CD) tolerance improvements of the filter bank multicarrier (FBMC) over orthogonal frequency division multiplexing (OFDM) for high-baudrate spectral slicing transmitter and single coherent receiver transmissions. For a 512 Gb/s 16 quadrature amplitude modulated (16QAM) spectrum slicing system at 1600 km of fiber transmission, the FBMC-based system reduces TE and residual CD penalties by more than 1.5 dB and 3 dB, in comparison to the OFDM-based system, respectively.

Index Terms: Multicarrier, coherent optical orthogonal frequency division multiplexing (OFDM), spectrum slicing, spectrum engineering, filter bank multicarrier (FBMC), delay mismatch, timing error, delay lines.

1. Introduction

To meet the rapidly increasing demand for capacity, high spectral efficiency (SE) systems with cost-effective implementations have gained a lot of attention recently [1]–[4]. The concept of superchannel has been proposed to push the data rate per interface up to the order of Tb/s [1], [5]. Moreover, due to the high bandwidth of commercially available photodiodes, superchannel can be effectively received and processed by a single coherent receiver, leading to a significant reduction in the overall cost per bit. However, up to now, it is still very challenging to generate superchannels with over 100 GHz of bandwidth using a single in-phase quadrature (IQ) optical modulator. As a result, alternative approach such as spectral slice (SS) engineering of the spectrum [2]–[4] has been proposed to generate high-baudrate superchannel signals. The report in [2] demonstrates a record symbol rate of 127.9 Gbaud 16QAM with the implementation of Nyquist-pulse shaping and spectrum slicing synthesis techniques. However, in this work, a Q-factor penalty of around 7 dB was observed. This penalty was due to the imperfect receiver and the timing mismatch (timing error) among optical paths, which always exists before the coupling of spectral slices at the transmitter. As a result, in [2], delay lines (DLs) were required to keep the timing mismatch below 1 ps

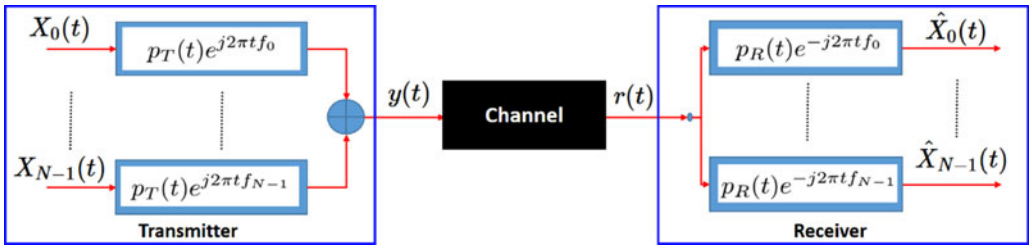

Fig. 1. Principle transmission diagram of a multicarrier system.

for the Nyquist-pulse shaping. Such timing-mismatch requirement is very challenging for practical implementation and thus, alternative modulation formats with higher tolerance to timing mismatch among optical paths are highly desirable for high-baudrate superchannel transmissions.

In general, due to the long symbol duration, it is naturally expected that multicarrier signals are more tolerant to timing mismatch in comparison to single carrier signal. Multicarrier modulation formats, such as orthogonal frequency division multiplexing (OFDM), have been considered as potential techniques for the application of high speed, long-haul, and multi-wavelength optical networks due to the capability of inter-symbol interference (ISI) mitigation using simple digital signal processing (DSP) techniques [1], [6]. However, to the best of our knowledge, OFDM has not yet been studied for SS systems where the whole bandwidth is received and processed by a single coherent receiver, taking advantages of the high-bandwidth photodetectors. In OFDM transmissions, timing mismatch among optical paths not only leads to intercarrier interference (ICI) but also increases the synchronization error, which can degrade significantly the system performance. To mitigate the impact of timing mismatch among optical paths we also consider here filter bank multicarrier (FBMC)-an evolution of OFDM in which the rectangular pulse shaping is replaced by a modified raised cosine filtering.

In this paper, we study the application of multicarrier techniques i.e. OFDM and FBMC for a SS system of 128 Gbaud 16QAM (leading to a total of 512 Gb/s for a single polarization) with a single coherent receiver. For the first time, the impact of timing mismatch in the multicarrier SS systems has been investigated. The comparison of OFDM and FBMC was provided in terms of timing error (TE) (also called delay mismatch (DM)) and residual chromatic dispersion (CD) tolerances. We numerically demonstrated that the impact of the DMs and delay spreads due to residual CD on the SS system could be effectively mitigated by employing FBMC.

2. Fundamentals of Multicarrier Techniques: OFDM and FBMC

Both OFDM and FBMC inherit the same principle of multicarrier transmission systems (see Fig. 1). The transmitted signal $y(t)$ is the sum of the signals on all channels (or subcarriers) and given as

$$y(t) = \sum_{k=0}^{N-1} \sum_{\rho=-\infty}^{+\infty} X_{k,\rho} p_T(t - \rho T_s) e^{j2\pi t f_k} \tag{1}$$

where $X_{k,\rho}$ is the data on the k^{th} subcarrier at the ρ multicarrier symbol, f_k is the carrier frequency of the k^{th} subcarrier, N is the number of subcarriers, T_s is the multicarrier symbol period, and $p_T(t)$ is the prototype filter (PF) at the transmitter which is normally designed once for all subcarriers. The term $p_T(t - \rho T_s)e^{j2\pi t f_k}$ implies that the PF at the k^{th} subcarrier in the ρ^{th} symbol can be regarded as the time delay - frequency shifted version of the same prototype low-pass filter $p_T(t)$. If we sample the transmitted signal at the sample rate of N/T_s, the simplified discrete transmitted signal from (1) can be rewritten as

$$y[n] = \sum_{k=0}^{N-1} \sum_{\rho=-\infty}^{+\infty} X_{k,\rho} p_T[n - \rho N] e^{j\frac{2\pi}{N} n T_s f_k}. \tag{2}$$

The difference between OFDM and FBMC originates from the PF design. For OFDM, the PF is simply a rectangular pulse during a symbol period, i.e. $p_T(t) = \text{const.}, 0 \leqslant t < T_s$ while it is typically a modified raised cosine, root-raised cosine or root Nyquist in the case of FBMC [7]. To maximize the signal-to-noise ratio (SNR) at the receiver, the matched filtering configuration is utilized, i.e. $p_R(t) = p_T(-t)$ [7]. The recovered symbols will be separated without ISI if the following orthogonality condition is satisfied [7]:

$$< p_{T,k}(t - mT_s), p_{R,l}(t - nT_s) >= \int_{-\infty}^{+\infty} p_{T,k}(t - mT_s) p^*_{R,l}(t - nT_s) dt = \delta_{l,k}\delta_{m,n} \tag{3}$$

where $p_{T,k}(t) = p_T(t)e^{j2\pi t f_k}$, and $p_{R,l}(t) = p_R(t)e^{j2\pi t f_l}$. The $*$ denotes complex conjugate operator and $\delta_{l,k}$ is the Kronecker function. To satisfy the orthogonality, f_k is chosen so that $f_k T_s = k$. Substitute f_k into (2), the simplified discrete transmitted signal $y[n]$ can be rewritten as

$$y[n] = \sum_{k=0}^{N-1} \sum_{\rho=-\infty}^{+\infty} X_{k,\rho} p_T[n - \rho N] e^{j\frac{2\pi}{N}nk}. \tag{4}$$

2.1 OFDM Modulation/Demodulation

By choosing the rectangular PF in OFDM, i.e., $p_T(t) = \frac{1}{\sqrt{N}}, 0 \leqslant t < T_s$, the OFDM symbols are isolated in the time domain. Thus, we can analyze only one OFDM symbol and the discrete baseband OFDM signal $y[n]$ in one symbol period is rewritten from (4) with the rectangular PF substitution as

$$y[n] = \frac{1}{\sqrt{N}} \sum_{k=0}^{N-1} X_k e^{j\frac{2\pi}{N}nk} = \mathcal{F}^{-1}(X_k), \quad 0 \leqslant n < N. \tag{5}$$

Thus, a set of orthogonal subcarriers can be easily generated by employing the inverse fast Fourier transform (iFFT) digital signal processing. This is the most significant advantage of OFDM, especially when the number of subcarriers is substantial. At the receiver side with ideal channel assumption, the recovered QAM symbols $\hat{X}_k$ can be obtained easily by employing the fast Fourier transform (FFT) algorithm with respect to the received signal $r[n]$

$$\hat{X}[k] = \mathcal{F}(r[n]) = \frac{1}{\sqrt{N}} \sum_{n=0}^{N-1} r[n] e^{-j\frac{2\pi}{N}nk}, \quad 0 \leqslant k < N. \tag{6}$$

2.2 FBMC Modulation/Demodulation

For the FBMC, the PF is not a constant pulse but a modified cosine shape and it lasts for several symbol duration. In our investigation, we adopted the PF from the FP7 European research project PHYDYAS [8] for the FBMC implementation. The PF is characterized by two parameters: filter's length L and oversampling factor $K = L/N$. It was pointed out in [8] that the factor $K = 4$ is optimum for high-speed transmission in terms of the trade-off between performance and complexity. The filter coefficients of PF in frequency domain were obtained in [8] as $P_0 = 1$, $P_{\pm 1} = 0.97196$, $P_{\pm 2} = \sqrt{2}/2$, and $P_{\pm 3} = 0.235147$. The corresponding impulse response of PF can therefore be determined by applying the iFFT to the frequency response, which yields

$$\begin{aligned} p[m] &= 1 + 2\sum_{k=1}^{K-1} (-1)^k P_k \cos\left(\frac{2\pi k}{NK} m\right), \quad m = 1, ..., L-1 \\ p[0] &= 0. \end{aligned} \tag{7}$$

The PFs impulse and frequency responses comparisons of the OFDM (the rectangular pulse) and FBMC (the PHYDYAS pulse) with the number of subcarriers of 16 ($N = 16$) and the overlapping factor of 4 ($K = 4$) are shown in Fig. 2. Clearly, the impulse response duration of FBMC is K times, i.e. 4 times, longer than OFDMs and the out-of-band power leakage of FBMC is much

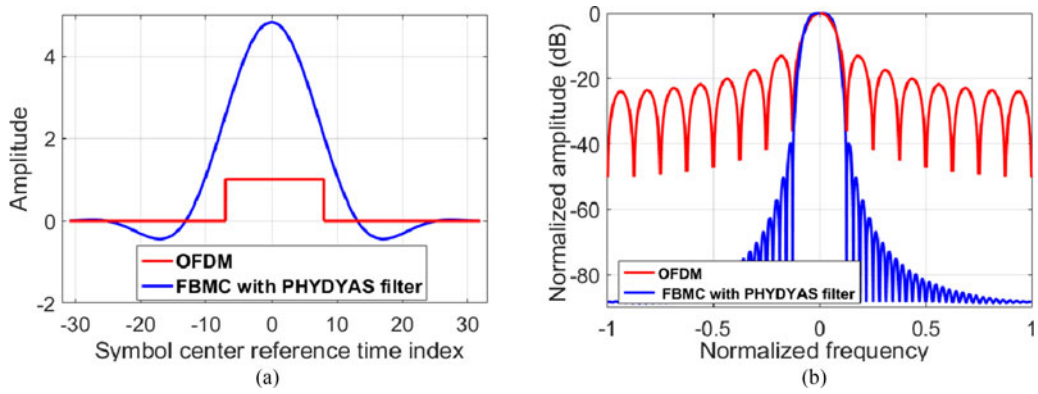

Fig. 2. Impulse and frequency responses comparison of OFDM and PHYDYAS FBMC. (a) Impulse response comparisons. (b) Frequency response comparisons.

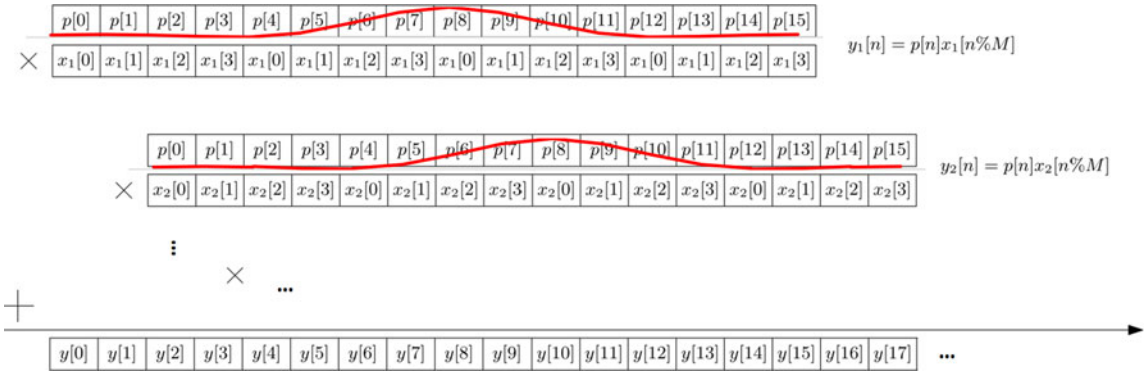

Fig. 3. Filter bank synthesis PPN-based procedure at the transmitter.

lower than that of OFDM. These features will make FBMC more robust than OFDM regarding the timing problems, delay spreads and frequency offset error as well. Nevertheless, the PHYDYAS PF described by (7) only guarantees the orthogonality in real fields [8], [9]. Therefore, only real values are modulated in FBMC. The real and the imaginary parts of a complex data symbol are not modulated simultaneously but the imaginary part is delayed by the half symbol duration. In order to maintain the same SE as in OFDM, the offset QAM (OQAM) is normally employed with the symbol time spacing being reduced by a factor of two.

In general, frequency spreading (FS) or poly-phase network (PPN) technique can be used to realize the FBMC [8]. In our consideration, the PPN was chosen because it provides the same number point of iFFT/FFT as in OFDM and lower complexity than FS [8]. Since only the real valued symbols are modulated, the iFFT/FFT implementation in FBMC needs to run at twice the speed as in OFDM to keep the same throughput as in OFDM counterpart. After the iFFT operation, the FBMC signal can be synthesized at the transmitter side with the so-called filter bank synthesis (FBS) via two steps as illustrated in Fig. 3 [10]: 1) frame duplication and multiplication and 2) half-symbol overlap and sum. The transmitted FBMC signal $y[n]$ after the synthesis filtering can be written as

$$y[n] = \sum_{\rho=1}^{K} y_\rho \left[n - \frac{\rho - 1}{2} N \right] \tag{8}$$

where $y_\rho[n] = p[n]x_\rho[n\%N]$ is the output of the frame ρ. The % denotes the remainder operator. x_ρ is the ρ^{th} frame of K-time duplicate version of the signal after iFFT of the ρ^{th} frame OQAM

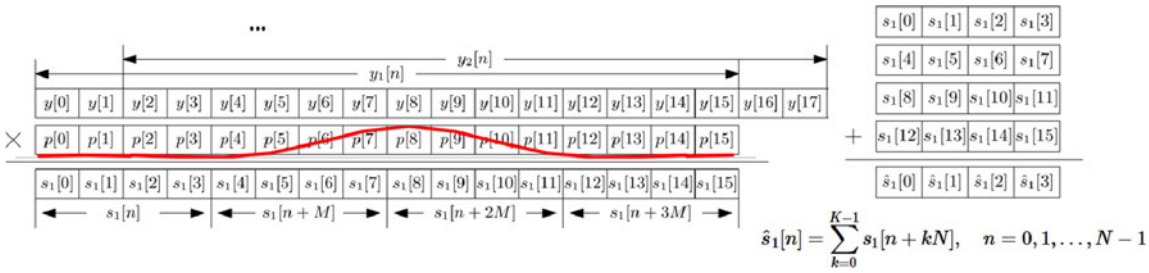

Fig. 4. Filter bank analysis PPN-based procedure at the receiver.

input X_ρ

$$x_\rho[n] = \mathcal{F}^{-1}(X_\rho[k]) = \frac{1}{\sqrt{N}} \sum_{k=0}^{N-1} X_\rho[k] e^{j\frac{2\pi}{N}nk}, \quad 0 \leqslant n \leqslant N-1. \tag{9}$$

At the receiver side, the incoming signal is first processed by the so-called filter band analysis (FBA). Fig. 4 shows two processing steps in the FBA [10]: (1) frame grouping and multiplication, and (2) re-size and summing-up. The signal after these processes is written

$$\hat{s}_\rho[n] = \sum_{k=0}^{K-1} s_\rho[n+kN], \quad n = 0, 1, ..., N-1 \tag{10}$$

where $s_\rho[n] = p[n] r_\rho[n]$ is the output of the multiplication between the ρ^{th} frame and the PF impulse response. The $r_\rho[n]$ is the received signal at the ρ^{th} frame. With ideal channel assumption, i.e. $r[n] = y[n]$, the estimation of the transmitted OQAM symbols $\hat{X}_\rho$ can be recovered at this stage by an FFT operation

$$\hat{X}_\rho[k] = \mathcal{F}(\hat{s}_\rho[n]) = \frac{1}{\sqrt{N}} \sum_{n=0}^{N-1} \hat{s}_\rho[n] e^{-j\frac{2\pi}{N}nk}, \quad 0 \leqslant k \leqslant N-1. \tag{11}$$

3. Model Descriptions and Parameters

3.1 Multicarrier—Spectrum Slicing Synthesis at the Transmitter

Numerical simulation of the SS system with either OFDM or FBMC synthesis was performed by MATLAB v2016b. Fig. 5 depicts the transceiver block diagram of the SS system. In our model, we divided the total spectrum of approximately 130 GHz into five slices which were generated in parallel before multiplexing. The 16QAM 128 Gbaud superchannel signal was formed from five 16QAM 25.6 Gbaud slices. At the transmitter, either 25.6 Gbaud 16QAM OFDM or FBMC signal on each slice was synthesized and fed into a IQ modulator. We assumed that the five coherent spectral components which were fed into five corresponding IQ modulators were originated from an ideal external cavity laser (ECL) through an ideal comb generator. Their frequencies were approximately 26 GHz apart from each other.

The digital implementation procedures of OFDM and FBMC on each slice are shown in the insets of Fig. 5(A). We designed both OFDM and FBMC SS systems with the same number of 128 subcarriers in which 8 pilots were reserved for equalization. There are certain similarities between FBMC and OFDM since FBMC is evolved from OFDM with regard to PF design. This analogy can be seen clearly in Fig. 5(A). A filter bank synthesis module was added for FBMC while there was actually no PF processing for OFDM (OFDMs PF is simply a constant value for the whole OFDM symbol). The high rate source bits were transformed into multiple lower streams via serial-to-parallel module. They were then fed into a digital modulator to form complex QAM symbols (for the OFDM case) or OQAM symbols (for FBMC case) where each low-speed stream of symbols corresponds

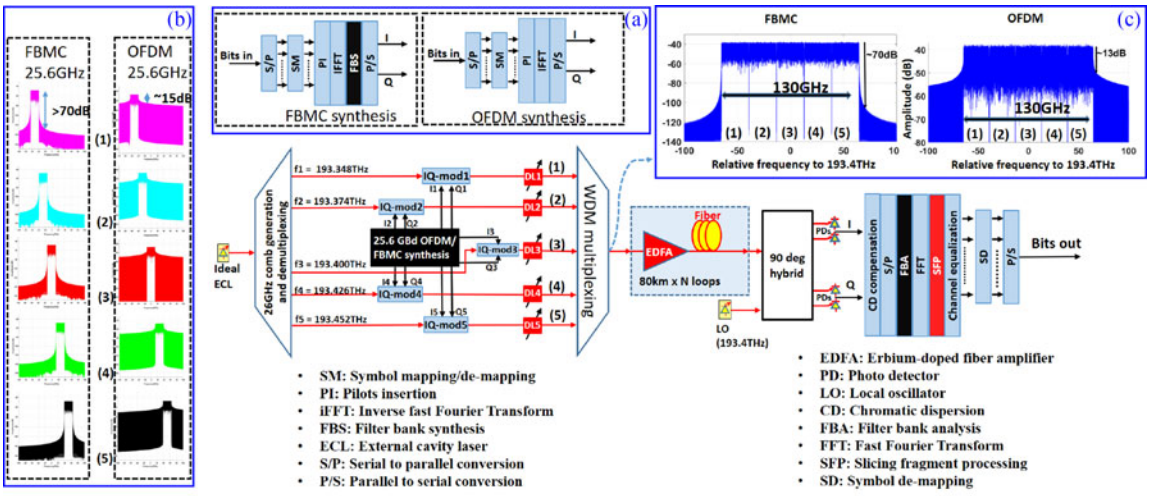

Fig. 5. Block diagram of spectrum slicing systems with either OFDM or FBMC synthesis. (a) Digital implementation procedure diagram of OFDM and FBMC. (b) Output spectrums of the OFDM and FBMC signals on five corresponding slices. (c) Transmitted spectrums of the OFDM and FBMC SS superchannel signal.

to one input of multicarrier modulator. Eight uniform pilots were inserted into the multicarrier symbol to aid the equalization at the receiver. All 128 complex symbols including pilots in frequency domain were then modulated on 128 subcarriers by the iFFT module, and they were converted to serial stream to form a multicarrier symbol in time domain for the OFDM. For FBMC, however, there was an extra process for filter bank synthesis (as discussed in Section 2) before the parallel-to-serial conversion. The in-phase (I) and quadrature (Q) components of the time-domain multicarrier symbol were finally used to drive the IQ modulator. The input optical carriers on five IQ modulators are 193.348 THz, 193.374 THz, 193.400 THz, 193.426, THz, and 193.542 THz, respectively. The output spectra of the OFDM and FBMC signals on the five corresponding slices are shown in Fig. 5(b). Before coupling, the DLs were added to synchronize optically the signal on the slices. At the output of the multiplexing, the 128 Gbaud 16QAM superchannel signal was formed from the signals on five slices. The superchannel signal was then launched into the fiber channel for transmitting. The transmitted spectra of the OFDM and FBMC superchannel signals are shown in Fig. 5(c).

3.2 Fiber Channel Modeling

The electric field complex envelop of a traveling light wave can be mathematically described by the nonlinear Schrödinger equations [11]. Herein, we utilized the symmetric split-step Fourier method to model the fiber channel in which the link was divided into several sections. Within each section, the mathematical solution to the nonlinear Schrödinger equation is approximated by [11]

$$E(z+h,t) \approx \exp\left(\frac{h}{2}\hat{D}\right)\exp\left(h\hat{N}\left[E\left(z+\frac{h}{2},t\right)\right]\right)\exp\left(\frac{h}{2}\hat{D}\right) \tag{12}$$

where $E(z, t)$ denotes the electric field complex envelop of the light wave at the distance z and time t, and h is the step-size. $\hat{D} = \frac{-j\beta_2}{2}\frac{\partial^2}{\partial t^2} - \frac{\alpha}{2}$ and $\hat{N} = j\gamma \mid E \mid^2$ are the linear and nonlinear operators, respectively. β_2 describes the first-order group velocity dispersion, α is the fiber attenuation, and γ is the nonlinear Kerr coefficient.

In our simulation, a transmission link of up to 24 spans of standard single mode fiber (SSMF) with 80 km span- length was considered. We fixed the step-size, h, of 1 km for the fiber modeling. Following parameters of the SSMF are $\alpha = 0.2$ dB km^{-1}, $\beta_2 = -2 \times 10^{-26}$ S^{2}M^{-1} at the wavelength of 1550 nm (corresponding to the fiber dispersion of 17 ps km nm^{-1}), and $\gamma = 1.2$ W km^{-1}. For each

span, an in-line simple Erbium-doped fiber amplifier (EDFA) with a gain of 16 dB and noise figure (NF) of 6 dB was used to compensate for the fiber attenuation.

3.3 Single Coherent Receiver

At the receiver side, the incoming optical superchannel signal was first converted into the equivalent baseband signal in electrical domain by a high-bandwidth coherent receiver. Conventional signal processing algorithms in the digital domain such as CD compensation, serial to parallel conversion, filter bank analysis (only with FBMC), FFT, slicing segment processing, channel equalization, symbol de-mapping and parallel to serial conversion were performed to recover the transmitted bits. The output bit sequence was then compared to the input bits from five slices at the transmitter to count the bit error rate (BER). For convenience, the equivalent Q-factor ($Q\,(dB) = 20\log_{10}[\sqrt{2}\,\mathrm{erfc}^{-1}(2BER)]$) was used to evaluate the systems performance. Common BER threshold before forward error correction (FEC) for 16QAM is 10^{-3} (equivalent Q-factor of 9.8 dB).

4. Results and Discussion

4.1 Back-to-Back Configuration

For the back-to-back configuration, the performances of single carrier and multicarrier systems are identical in term of SNR [10], [12]. Therefore, the BER expectations for both OFDM and FBMC rectangular QAM SS systems can be expressed as [13]

$$BER_{\mathrm{MQAM}} = \frac{2}{k}\left(\frac{\sqrt{M}-1}{\sqrt{M}}\right)\mathrm{erfc}\left(\sqrt{\frac{3k\gamma_b}{2(M-1)}}\right), \tag{13}$$

where M is the constellation size of the rectangular QAM, $k = \log_2(M)$ is the number of bits per symbol, and γ_b is the SNR per bit. It should be noticed that the equivalent optical SNR ($OSNR$) in one polarization with respect to the SNR per bit γ_b is

$$OSNR = \frac{R_b}{2B_{\mathrm{ref}}}\gamma_b \tag{14}$$

where R_b is the bit rate, and B_{ref} is the reference bandwidth, which is commonly chosen as 12.5 GHz.

Fig. 6 shows the TE tolerance comparisons of the OFDM and FBMC SS systems in the back-to-back configuration. The theoretical Q-factor expectation versus $OSNR$, which was derived from (13) and (14), is also provided. The TEs varied from 30.5 ps (case 1) to 122 ps (case 2), corresponding from $\sim$78 % to $\sim$310 % of the elementary symbol period ($\sim$39 ps). For both systems, the lower-bound performances when the DLs on all slices reach the maximum TE, i.e. 30.5 ps in case 1 or 122 ps in case 2, were compared. While the Q-factor penalty of the SS system with FBMC was negligible ($<$0.5 dB) at the TEs of 30.5 ps, its penalty with OFDM was considerable, increasing dramatically from 1.0 dB to 6.5 dB at the $OSNR$ of 20 dB and 32 dB, respectively. When the TEs increased to 122 ps, the performance of SS system with OFDM distorted severely while there was just 2.5 dB Q-factor penalty of the systems with FBMC at the same $OSNR$ of 26 dB.

4.2 Long-Haul Transmission

We conducted simulations with the long-haul optical transmission and investigated the impact of the DLs mismatch phenomenon and residual CD for the SS system with both OFDM and FBMC implementations. Firstly, the Q-factors versus launched optical powers for both systems were carried out as shown in Fig. 7, to search for the optimum launched power where the best of Q-factor was obtained. The fiber transmission distance was fixed at 1120 km. The performance of separate slices and the average performance are also plotted for both OFDM and FBMC SS systems. Clearly, the average performances of two SS systems were almost identical although there were some minor differences in separate slice performance comparison between two systems. Because there was

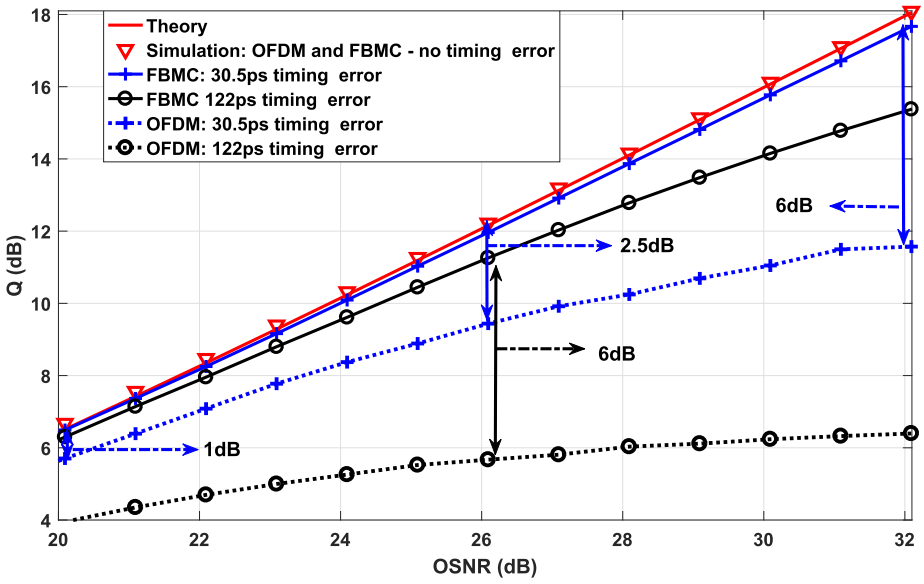

Fig. 6. Delay mismatches tolerances comparison between the FBMC and OFDM SS systems with back-to-back configuration.

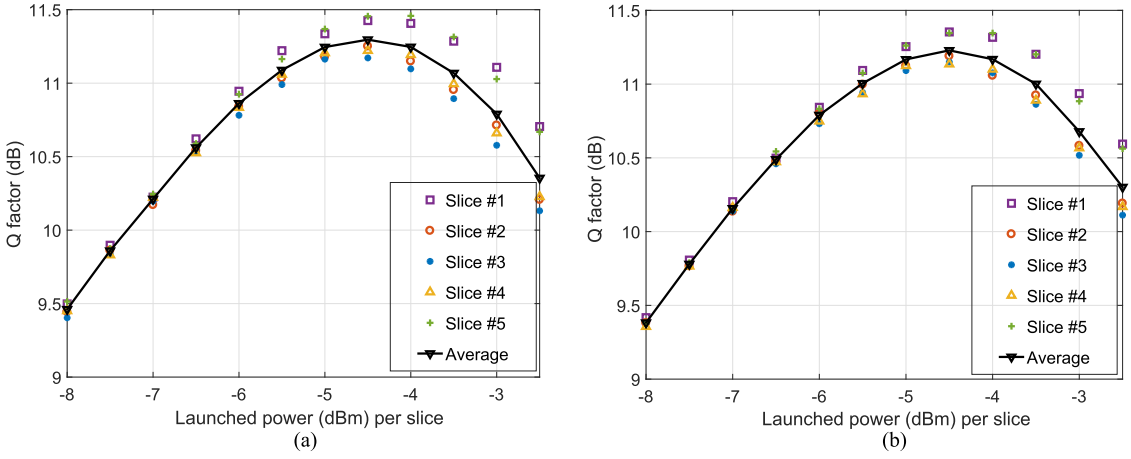

Fig. 7. Performance of the OFDM and FBMC SS systems versus launched power at the transmission distance of 1120 km. (a) OFDM SS system. (b) FBMC SS system.

no timing error, frequency error, or CD residual for this case study, the performance of FBMC should not differ from OFDM counterpart. These expected outcomes verify the validity of the developed theoretical models. The optimum launched power for both SS systems was around -4.5 dBm.

Secondly, we studied the TE and residual CD tolerance of both SS systems for different transmission distances at the obtained optimum launched power of -4.5 dBm. The results in Fig. 8(a) reveal an excellent TE tolerance of the FBMC SS system over OFDM SS system. In perfect conditions, both systems obtain the same performances for the transmission distance of up to 1600 km with BER below the FEC threshold. Nevertheless, the performance of the OFDM SS system degraded dramatically if all slices were not synchronized optically while there was just a small amount of performance penalty of the system with FBMC counterpart. We changed the DLs mismatch from 30.5 ps to 122 ps as in our previous study. For the same transmission distance of 1600 km, at the TE of 30.5 ps and 122 ps, we observed Q-factor penalties of almost 0.0 dB and 0.5 dB, respectively

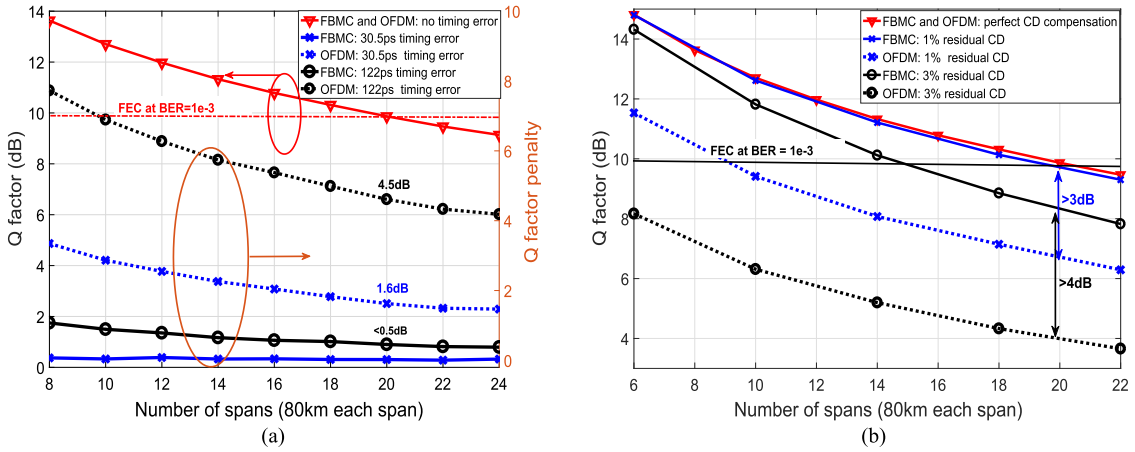

Fig. 8. Performance comparisons of the ODFM SS system versus the FBMC SS system at the optimum launched power of −4.5 dBm. (a) Timing error tolerance versus transmission distance. (b) Residual chromatic dispersion tolerance versus transmission distance.

for the system with FBMC while these respective values of the system with OFDM were ∼1.6 dB and ∼4.5 dB. The same residual CD tolerance improvement of the SS system with FBMC over with OFDM was obtained in Fig. 8(b). The CD is normally not perfectly compensated in practice. The obtained results showed that the FBMC SS system was also more robust to the residual CD than OFDMs by 3 dB and 4 dB at 1 % and 3 % of the residual CD, respectively. This comes from the fact that the FBMC PFs impulse response is four times longer than the OFDMs.

5. Conclusion

For the first time, we have implemented the multicarrier-based 128 Gbaud 16QAM SS systems for the long-haul transmission distance. We evaluated and compared the performance of the SS system with OFDM and FBCM in different configurations by numerical simulations. The results showed that the FBMC-based SS system was superior to the OFDM based SS system in terms of robustness to the timing errors and delay spreads at the cost of slightly increasing the complexity. FBMC, therefore, would be a very potential candidate for spectral slice engineering applications in the future.

References

[1] S. Chandrasekhar and X. Liu, "OFDM based superchannel transmission technology," *J. Lightw. Technol.*, vol. 30, no. 24, pp. 3816–3823, Dec. 2012.
[2] H. Mardoyan, M. A. Mestre, P. Jennevé, L. Schmalen, A. Ghazisaeidi, and P. Tran, "Transmission of single-carrier Nyquist-shaped 1-Tb/s line-rate signal over 3,000 km," in *Proc. Opt. Fiber Commun. Conf.*, no. 1, 2015, pp. 3–5.
[3] J. Renaudier, P. Brindel, H. Mardoyan, P. Jennevé, L. Schmalen, and G. Charlet, "1-Terabit/s net data-rate transceiver based on single-carrier Nyquist-shaped 124 GBaud PDM-32QAM," in *Proc. Opt. Fiber Commun.*, no. 1, pp. 1–3, 2015.
[4] D. S. Millar *et al.*, "Design of a 1 Tb/s superchannel coherent receiver," *J. Lightw. Technol.*, vol. 34, no. 6, pp. 1453–1463, Mar. 2016.
[5] Y. Zhu *et al.*, "Experimental comparison of Terabit Nyquist superchannel transmissions based on high and low baud rates," in *Proc. Opt. Fiber Commun. Conf./Nat. Fiber Opt. Eng. Conf. 2013*, 2013, Paper JW2A.37.
[6] J. Armstrong, "OFDM for optical communications," *J. Lightw. Technol.*, vol. 27, no. 3, pp. 189–204, Feb. 2009.
[7] A. Sahin, I. Guvenc, and H. Arslan, "A survey on multicarrier communications: Prototype filters, lattice structures, and implementation aspects," *IEEE Commun. Surveys Tut.*, vol. 16, no. 3, pp. 1312–1338, Jul.–Sep. 2014.
[8] M. Bellanger, "FBMC physical layer: A primer," PHYDYAS EU FP7 Project, pp. 1–31, Jan. 2010. [Online]. Available: http://www.ict-phydyas.org/teamspace/internal-folder/FBMC-Primer_06-2010.pdf.
[9] R. M. R. Nissel, "On pilot-symbol aided channel estimation in FBMC-OQAM," *Proc. IEEE Int. Conf. Acoust., Speech Signal Process.*, 2016, pp. 3681–3685.

[10] Q. He and A. Schmeink, "Comparison and evaluation between FBMC and OFDM systems," in *Proc. 19th Int. ITG Workshop Smart Antennas*, 2015, pp. 1–7.
[11] O. V. Sinkin, R. Holzlöhner, S. Member, J. Zweck, and C. R. Menyuk, "Optimization of the Split-Step Fourier Method in Modeling Optical-Fiber Communications Systems," *J. Lightw. Technol.*, vol. 21, no. 1, pp. 61–68, Jan. 2003.
[12] E. Ip, A. P. T. Lau, D. J. F. Barros, and J. M. Kahn, "Coherent detection in optical fiber systems," *Opt. Exp.*, vol. 16, no. 2, pp. 753–791, 2008. [Online]. Available: http://www.opticsexpress.org/abstract.cfm?URI=oe-16-2-753.
[13] R.-J. Essiambre, G. Kramer, P. J. Winzer, G. J. Foschini, and B. Goebel, "Capacity limits of optical fiber networks," *J. Lightw. Technol.*, vol. 28, no. 4, pp. 662–701, Feb. 2010.